Astron. Astrophys. 325, 329–340 (1997)

ASTRONOMY
AND
ASTROPHYSICS

Wave heating of coronal loops driven by azimuthally polarised footpoint motions

II. The time-dependent behaviour in ideal MHD

W.J. Tirry[⋆] **and D. Berghmans**[*]

Centre for Plasma Astrophysics, K.U. Leuven, Celestijnenlaan 200 B, B-3001 Heverlee, Belgium

Received 17 January 1997 / Accepted 10 March 1997

Abstract. We study the heating of coronal loops by linear resonant Alfvén waves that are excited by photospheric footpoint motions of the magnetic field lines. The analysis is restricted to azimuthally polarised footpoint motions so that Alfvén waves are excited directly. At the radii where Alfvén waves, travelling back and forth along the length of the loop, are in phase with the footpoint motions, the oscillations grow unbounded in ideal MHD. In the companion paper (Paper I) dissipation is included and we looked at the steady state in which the energy injected at the photospheric part of the loop is balanced by the energy dissipated in the dissipative layer around the resonance. In this paper we make an analysis in time-dependent ideal linear MHD in order to get more physical insight in the results of Paper I and to get information about the time scales involved.

In the present study the azimuthal wave number is taken to be non-zero so that Alfvén and fast wave do not exist independently. In this case the heating in the resonance layer becomes a complicated interplay of the influence of the Alfvén waves excited directly at the photospheric base of the resonant layer and the influence of the quasi-modes excited indirectly. We find that the presence of these quasi-modes influence the resonance development dramatically. This is unexpected, since in contrast to a sideways driven loop, a loop driven at the footpoints by azimuthally footpoint motions does not need quasi-modes as energy carrier waves.

Key words: MHD – Sun: corona – Sun: magnetic fields-waves – methods: analytical

1. Introduction

The solar corona consists of highly inhomogeneous plasma with a temperature of roughly 3×10^6 K. This temperature is a few orders higher than the underlying photospheric temperature, indicating the presence of heating mechanisms. Since Skylab it is known that the largest contribution to the X-ray emission and to the heating of the solar corona comes from loop like structures in the solar atmosphere. These magnetic loops are viewed as the basic building blocks of the solar corona. The high conductivity and the relatively high mass density of the photospheric plasma provide an effective photospheric anchoring of the magnetic field lines. The photospheric footpoints of the magnetic field lines are forced to follow the convective motions. If these footpoint motions are slow (in comparison with the Alfvénic transit time along the loop), the coronal flux tubes are twisted and braided, which builds up magnetic stresses and leads to the formation of small length scale by the creation of field discontinuities (Parker 1972) or by cascade of magnetic energy to very small length scales (Van Ballegooijen 1985). These mechanisms to generate small length scales, and hence heating, are usually classified as DC heating mechanisms (Zirker 1993).

In contrast, footpoint motions which are 'fast' in comparison with the Alfvénic transit time, generate magnetosonic waves and Alfvén waves. Due to the steep density gradients at the photospheric edges these MHD waves reflect back and forth along the length of the loop. The loop is then expected to act as a leaking, resonant cavity for MHD waves (Hollweg 1984). Observational evidence of MHD waves propagating in coronal loops has indeed been reported. The UV spectrum suggests nonthermal velocities of 10-20 km/s (Cheng, Doschek & Feldman 1979). Recent studies of soft X-ray lines from the XRP indicate nonthermal motions of 30-40 km/s above active regions (Saba & Strong 1991).

An important property of MHD waves in an inhomogeneous plasma is that a global wave motion can be in resonance with local oscillations of a specific magnetic surface. The resonance condition is that the frequency of the global motion is equal to either the local Alfvén or the local cusp frequency of the magnetic surface. In this way energy is transferred from the large scale motion to oscillations which are highly localised to the neighbourhood of the Alfvén or cusp singular surface. In dissipa-

Send offprint requests to: W.J. Tirry

[⋆] Research Assistant of the F.W.O.-Vlaanderen

tive MHD this behaviour is mathematically recovered as eigenmodes which are exponentially damped in time. Due to their global character (oscillating with the same frequency throughout the plasma) these modes are called 'global modes'. For ideal MHD such a damped oscillation cannot be an eigenmode of the system, and for this reason they are often called 'quasi-modes' (see Tirry & Goossens 1996 and references therein). A lot of work, both analytically and numerically, was done on sideways excitation where a wave impinges laterally on the loop (Poedts et al. 1989; Poedts & Kerner 1992; Steinolfson & Davila 1993; Ofman & Davila 1995, 1996; Wright & Rickard 1995). Such an impinging MHD wave must necessarily be a fast wave since Alfvén waves cannot transport energy perpendicular to the magnetic field and slow waves are negligible in the corona due to the low gas pressure. When a loop is perturbed by a broad band spectrum on its side surface, it will respond at a discrete set of frequencies of fast waves which may resonantly excite Alfvén waves in turn. Hence the plasma-driver coupling was found to be very efficient due to the effect of the present global modes (Wright & Rickard 1995).

However it is important to see that sideways excitation by an externally impinging fast wave can only yield a minor contribution to the heating of a coronal loop by resonant absorption. Due to the enhanced density the interior Alfvén speed must be smaller than the exterior Alfvén speed. Therefore only fast waves which are exponentially decaying on their way to the loop can resonantly excite Alfvén waves inside the loop. This suggests that fast waves originating from within the loop must be the prime contribution. Such fast wave can be excited by e.g. a reconnection event inside the loop or by the photospheric motions of the footpoints of the magnetic field lines.

The photospheric excitation of resonant waves has been subject to criticism. Here the important question arises whether the photosphere in fact offers sufficient power at the right frequencies. Parker (1992) argues that the involved time scale, corresponding to the turn-over-time of the individual granules, is much too long. But as pointed out by Goedbloed (1994) a mechanism, similar to the stick slip mechanism that makes it possible for the violinist to excite frequencies of 200 Hz to more than 2000 Hz by a several orders of magnitude lower periodic motion of the bow, might overcome this problem. However such an equivalent mechanism has not been found yet.

As discussed in the overview on heating mechanisms by Zirker (1993), the observations available so far are not sufficiently detailed to either exclude or confirm the generation of large enough wave fluxes in the photosphere. Very promising in this context are the recent observations by Ulrich (1996) who reported magnetic oscillations in the photosphere which were identified as outgoing Alfvén waves with substantial power at low frequencies.

Recent observations by Falconer et al. (1996) suggest that microflaring might directly heat the coronal plasma in the sheared local core field and generate waves that propagate into extended loops and dissipate there to produce the enhanced coronal heating in the bodies of these larger structures. The frequency spectrum of the waves by the network "microflares" is of considerable interest. Since the periods of the waves that result from magnetic reconnection events are determined by the Alfvén speed and the geometry of the magnetic configuration involved, they do not suffer from the criticism by Parker. The reconfiguration of the magnetic field associated with a microflare converts very low frequency motions acting over a long time to high frequency motions generated over a short time.

Furthermore the theoretical investigation on footpoint excitation of MHD waves has only recently been reported. This problem involves the explicit solution of the wave-dynamics not only in the radial direction, but also in the longitudinal direction in order to include the appropiate boundary conditions at the loop's feet. Due to the intrinsic difficulty of the footpoint driven problem, authors have often assumed the azimuthal wave number to be zero in order to avoid complications with the coupling of quasi-modes and Alfvén waves (Heyvaerts & Priest 1983; Berghmans & De Bruyne 1995; Berghmans, De Bruyne and Goossens 1996; Poedts & Boyton 1996; Ruderman et al. 1996). A remarkable exception to this restriction has been the work by Halberstadt & Goedbloed (1995a,b). They calculated the stationary state solutions in the case of footpoint excitation of Alfvén waves and in the case of an external surface excitation source at the ends of the loop. Their results leave little doubt: the coupling of the global mode to the localized Alfvén wave strongly increases the dissipation rate in the vicinity of the eigenfrequency of the quasi-modes. Poedts, Beliën & Goedbloed (1994) showed that the resonances (by sideways excitation) in coronal loops have bad quality (the quality Q of a resonance is defined as the ratio of the total energy contained in the system to the dissipation per driving cycle). This means a lot of Ohmic heating per driving cycle compared to the total energy stored in the loop. As a consequence, they conclude that the time scales of the heating process can be relatively short and resonant absorption turns out to be a viable candidate for the heating of the magnetic loops observed in the solar corona.

In a paper which is rather related to the present one, Tirry, Berghmans & Goossens (1997) studied the temporal evolution of linear MHD waves excited by radially polarised footpoint motions. In this case only fast waves are driven directly, including the quasi-modes. They came to the conclusion that the resonant absorption of Alfvén waves indirectly excited by radially polarised footpoint motions through a global mode generates the small length scales necessary for coronal heating in acceptable time scales.

In the companion paper by Berghmans & Tirry (1997, hereafter referred to as Paper I) an analysis in the stationary state is adopted in order to determine the optimal footpoint motion parameters for heating by resonant excitation of Alfvén waves in coronal loops by azimuthally polarised footpoint motions. These authors found that the dependence of the heating on the driving frequency and the azimuthal wave number is drastically changed in presence of a quasi-mode.

The main topic of the present paper is a time-dependent study of resonant excitation of Alfvén waves in coronal loops that are generated by azimuthally polarised photospheric motions of the footpoints of the magnetic fieldlines in order to get

more insight in the steady state results of Paper I. This study also enables us to investigate how the phase-mixing length scale in time is affected by the coupling to the fast waves, and especially to the quasi-mode. It provides a step in the answer whether the development of resonance layers and the involved phase-mixing by this kind of footpoint motions are effective in producing the necessary dissipative small length scales on acceptably short time scales, consistent with the dissipative coefficients under the coronal conditions and with the observed length scales of the coronal loops.

We start in the next section by describing the slab geometry used to model a coronal loop. The relevant MHD equations and the underlying assumptions are discussed. Inspired by Berghmans, De Bruyne & Goossens (1996) we derive a formal analytic expression for the temporal evolution of the excited MHD waves as a superposition of eigenmodes (section 3a). To solve the corresponding eigenvalue problem we resort to the method described by Mann, Wright & Cally (1995). This approximative method, based on the truncation of a Fourier series, assures that the structure of the waves is fully resolved at any time (section 3b). The combination of the analytical findings and the numerical work yields an expression for the linear wave amplitudes at any point in 3D, and at any time as a result of the ongoing footpoint driving. In Sect. 4 we use this semi analytical/numerical expression to investigate, in close relationship with Paper I, how the coupling to the fast waves affects the temporal evolution of the resonant absorption and the associated phase-mixing. Sect. 5 is devoted to the influence of this coupling on the diffusion time scales. Finally in Sect. 6 we give a summary and discussion.

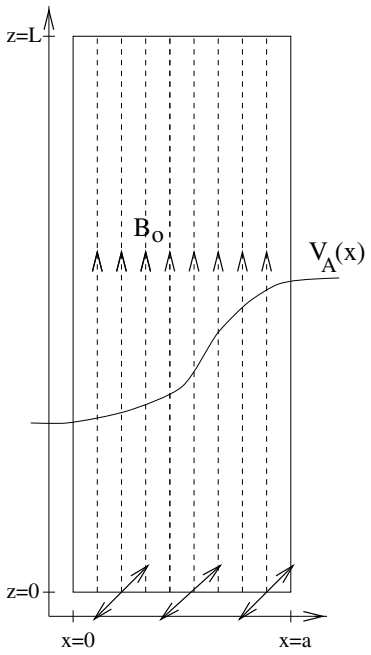

Fig. 1. A cartoon of the configuration used to model a coronal loop.

2. Physical model

A coronal loop is modelled as a static, straight plasma slab with thickness a, obeying the standard set of ideal MHD equations. Gravity is ignored. In the Cartesian coordinate system which we use, the x-coordinate corresponds to the radial direction, y-coordinate to the (ignorable) azimuthal coordinate and the z-coordinate represents the direction along the loop.

At $z = 0$ we impose a given footpoint motion whereas at $z = L$ we assume the loop to be line-tied. This can be done without any loss of generality because of the principle of superposition for solutions of linear equations. The boundary planes model the sharp transition from the corona to the photosphere (i.e. transition region, chromosphere and photosphere). We refer to these boundary planes as the 'photospheric edges' of the loop and we implicitly assume that a disturbance initiated in the photosphere indeed reaches the corona. In the radial direction we assume for mathematical tractability rigid wall conditions at $x = 0$ and $x = a$. We view $x = 0$ as the interior of the loop and $x = a$ as the exterior coronal environment.

The plasma is permeated by a uniform magnetic field ($\mathbf{B_0} = B_0\mathbf{e_z}$) and has a uniform pressure p_0 which we neglect in comparison with the magnetic pressure. Inhomogeneity of the plasma is introduced by a continuously varying density

$$\rho_0(x) = \rho_A + \rho_B \cos(\frac{\pi}{a}x) \qquad \text{with} \qquad \rho_B < \rho_A, \tag{1}$$

which models the higher density inside the loop. Fig. 1 shows a cartoon of the configuration used to model a coronal loop.

The fast modes corresponding to an eigenfrequency above the Alfvén continuum are travelling waves in the exterior coronal environment. In an open system these 'leaky' modes would radiate their energy away from the loop. In our closed box model of a coronal loop they are artificially kept in the neighbourhood of the loop. The modes with frequency within the range of the continuous spectrum (quasi-modes) are evanescent in the exterior coronal environment and thus correspond to body modes of the loop itself. Since we did not take into account a z-dependence of the density, our analysis is to be applied to coronal loops with their apex lower than one scale height.

The plasma is being shaken by small-amplitude perturbations at the footpoints of the magnetic field lines on the $z = 0$ plane. As long as non-linear and non-ideal effects are negligible we can follow the temporal evolution of the excited MHD waves inside the loop by solving the linear ideal MHD equations. The linear ideal MHD equations reduce for a pressureless plasma to

$$\{\frac{1}{v_A^2}\frac{\partial^2}{\partial t^2} - \frac{\partial^2}{\partial z^2} - \frac{\partial^2}{\partial x^2}\}\xi_x = \frac{\partial^2 \xi_y}{\partial y \partial x}, \tag{2}$$

$$\{\frac{1}{v_A^2}\frac{\partial^2}{\partial t^2} - \frac{\partial^2}{\partial z^2} - \frac{\partial^2}{\partial y^2}\}\xi_y = \frac{\partial^2 \xi_x}{\partial y \partial x}, \tag{3}$$

where ξ is the Lagrangian displacement and the Alfvén speed v_A is given by

$$v_A(x) = \sqrt{\frac{B_0^2}{\mu\rho_0(x)}}.$$

This coupled system of partial differential equations in ξ_x and ξ_y describes the coupled fast-Alfvén waves. Slow waves are absent ($\xi_z = 0$) because the plasma pressure is neglected.

Since the equilibrium quantities are constant in the y-coordinate which runs over an infinite interval, we can Fourier analyse with respect to y. For the Fourier component corresponding to wave number k_y, the time evolution and the spatial variation in x and z are described by

$$\{\frac{1}{v_A^2}\frac{\partial^2}{\partial t^2} - \frac{\partial^2}{\partial z^2} - \frac{\partial^2}{\partial x^2}\}\xi_x = ik_y\frac{\partial \xi_y}{\partial x}, \quad (4)$$

$$\{\frac{1}{v_A^2}\frac{\partial^2}{\partial t^2} - \frac{\partial^2}{\partial z^2} + k_y^2\}\xi_y = ik_y\frac{\partial \xi_x}{\partial x}. \quad (5)$$

Berghmans & De Bruyne (1995) and Berghmans, De Bruyne & Goossens (1996) simplified these equations by focussing on y-independent motions. In this case the fast and Alfvén waves are decoupled. Berghmans & De Bruyne give a fully analytical treatment of the time evolution of torsional Alfvén waves (corresponding to the ξ_y component as described by Eq. (5)). Berghmans, De Bruyne & Goossens extended the analysis to the sausage waves (corresponding to the ξ_x component as described by Eq. (4)) which are excited by radially polarised footpoint motions.

Tirry, Berghmans & Goossens derived an analytical expression describing the generation of linear MHD waves satisfying the coupled Eq. (4) and (5). In that paper only radially polarised footpoint motions are considered so that the resonant Alfvén waves are indirectly driven through coupling with the fast waves.

In this paper we focus on the excitation by azimuthally polarised footpoint motions. This means that Alfvén waves are directly driven and resonances are now due to the finite extent in the z-direction and through coupling with the fast waves. The influence of the coupling with fast waves on these resonances and the corresponding phase-mixing is investigated.

3. Mathematical approach

In this section we derive a formal analytical solution of the coupled equations (4) and (5) which describes the temporal evolution of linear MHD waves excited. The derivation is analogous to that by Tirry, Berghmans & Goossens (1997). The analysis is based on the papers by Mann, Wright & Cally (1995) and Berghmans, De Bruyne & Goossens (1996). Mann, Wright & Cally investigated the coupling of magnetospheric cavity modes to field line resonances. The matrix eigenvalue method that they used to follow the irreversible coupling between the fast magnetospheric cavity modes and the resonant Alfvén waves forms the basis of the numerical side of our approach. The second paper, by Berghmans, De Bruyne & Goossens, who considered the uncoupled Eq. for the fast waves, inspired the analytical approach which takes in a handy way the footpoint motions into account.

3.1. Formal analytical solution

We represent the footpoint motions by inhomogeneous boundary conditions for Eqs. (4) and (5) at the $z = 0$ and the $z = L$ boundary planes:

$$\begin{aligned}
\xi_x(x, y, z = 0, t) &= 0,\\
\xi_x(x, y, z = L, t) &= 0,\\
\xi_y(x, y, z = 0, t) &= R(x)T(t)e^{ik_y y},\\
\xi_y(x, y, z = L, t) &= 0.
\end{aligned}$$

We have assumed for mathematical simplicity that the dependencies on x and t of the footpoint motions are separable. In order to avoid complications with initial conditions we assume in addition that

$$\begin{aligned}
\xi_x(x, y, z, t = 0) &= \frac{\partial \xi_x(x, y, z, t = 0)}{\partial t} = 0,\\
\xi_y(x, y, z, t = 0) &= \frac{\partial \xi_y(x, y, z, t = 0)}{\partial t} = 0,
\end{aligned}$$

which leads to

$$T(t = 0) = \frac{\partial T(t = 0)}{\partial t} = 0 \quad (6)$$

Apart from these restrictions the functions $R(x)$ and $T(t)$ can be chosen completely arbitrarily. With the aid of the function (defined differently in comparison to the one used in Paper I)

$$\varphi(x, y, z, t) = i\xi_y(x, y, z, t) - (1 - \frac{z}{L})R(x)T(t)e^{ik_y y},$$

we include the footpoint motions as driving terms in the equations, while the boundary conditions become homogeneous

$$\{\frac{1}{v_A^2}\frac{\partial^2}{\partial t^2} - \frac{\partial^2}{\partial z^2} - \frac{\partial^2}{\partial x^2}\}\xi_x - k_y\frac{\partial \varphi}{\partial x} = \quad (7)$$
$$(1 - \frac{z}{L})k_y\frac{\partial R(x)}{\partial x}T(t),$$

$$\{\frac{1}{v_A^2}\frac{\partial^2}{\partial t^2} - \frac{\partial^2}{\partial z^2} + k_y^2\}\varphi + k_y\frac{\partial \xi_x}{\partial x} = \quad (8)$$
$$(1 - \frac{z}{L})(-k_y^2 - \frac{1}{v_A^2}\frac{\partial^2}{\partial t^2})R(x)T(t),$$

and

$$\xi_x(z = 0) = 0 = \xi_x(z = L), \quad \varphi(z = 0) = 0 = \varphi(z = L).$$

These homogeneous boundary conditions for ξ_x and φ now allow for the following sine-expansions

$$\begin{aligned}
\xi_x(x, y, z, t) &= \frac{2}{L}\sum_{n=1}^{\infty} X^{(n)}(x, y, t)\sin(\frac{n\pi}{L}z),\\
\varphi(x, y, z, t) &= \frac{2}{L}\sum_{n=1}^{\infty} Y^{(n)}(x, y, t)\sin(\frac{n\pi}{L}z).
\end{aligned}$$

The expansion of the function $(1 - \frac{z}{L})$ which appears in Eqs. (7) and (8) in a series of sines is

$$1 - \frac{z}{L} = \frac{2}{L}\sum_{n=1}^{\infty}\frac{L}{n\pi}\sin(\frac{n\pi}{L}z) \qquad \text{for } z \in]0, L], \tag{9}$$

where the righthandside is convergent to the lefthandside for all values of z but $z = 0$. This poses no difficulties since in what follows we only look for a weak solution. With the use of the sine-transforms the coupled partial differential Eqs. (7) and (8) are replaced by an infinite set of coupled partial differential equations for $X^{(n)}$ and $Y^{(n)}$. There is no coupling between different n-modes.

$$\{\frac{1}{v_A^2}\frac{\partial^2}{\partial t^2} + (\frac{n\pi}{L})^2 - \frac{\partial^2}{\partial x^2}\}X^{(n)} - k_y\frac{\partial Y^{(n)}}{\partial x} = \frac{L}{n\pi}k_y\frac{\partial R(x)}{\partial x}T(t), \tag{10}$$

$$\{\frac{1}{v_A^2}\frac{\partial^2}{\partial t^2} + (\frac{n\pi}{L})^2 + k_y^2\}Y^{(n)} + k_y\frac{\partial X^{(n)}}{\partial x} = \frac{L}{n\pi}(-k_y^2 - \frac{1}{v_A^2}\frac{\partial^2}{\partial t^2})R(x)T(t). \tag{11}$$

Since we are interested in the time evolution, a logical next step in the mathematical analysis is the application of the Laplace transformation

$$\hat{Q}(\omega) = \int_0^{\infty} Q(t)e^{i\omega t}dt,$$

$$Q(t) = \frac{1}{2\pi}\int_C \hat{Q}(\omega)e^{-i\omega t}d\omega,$$

where C is the Bromwich integration path running parallel to the real axis of the ω-plane above all singularities of $\hat{Q}(\omega)$. Application of this transformation to Eqs. (10) and (11) yields two coupled ODE for each n:

$$\{A[n] - \omega^2\}\begin{bmatrix}\hat{X}^{(n)}\\ \hat{Y}^{(n)}\end{bmatrix} = B[n] \tag{12}$$

where

$$A[n] = v_A^2\begin{bmatrix}(\frac{n\pi}{L})^2 - \frac{\partial^2}{\partial x^2} & -k_y\frac{\partial}{\partial x}\\ k_y\frac{\partial}{\partial x} & (\frac{n\pi}{L})^2 + k_y^2\end{bmatrix},$$

$$B[n] = \frac{L}{n\pi}v_A^2\hat{T}\begin{bmatrix}k_y\frac{\partial R}{\partial x}\\ (-k_y^2 + \frac{\omega^2}{v_A^2})R\end{bmatrix}.$$

The Eq. (12) can be solved by inversion of the operator $A[n] - \omega^2$. Formally this is not a problem, because $A[n]$ corresponds to the ideal MHD force operator which is Hermitian with respect to the following scalar product

$$< \xi_1|\xi_2 >= \int_0^a \xi_1\xi_2^*\rho dx. \tag{13}$$

It is well known that the eigenfunctions form a complete set so that the solution to Eq. (12) can be written as a spectral representation:

$$\begin{bmatrix}\hat{X}^{(n)}\\ \hat{Y}^{(n)}\end{bmatrix} = \sum_k \frac{1}{\omega_k^2 - \omega^2}|\psi_k^n >< \psi_k^n|B[n] > + \int \frac{1}{\sigma^2 - \omega^2}|\psi_\sigma^n >< \psi_\sigma^n|B[n] > d\sigma, \tag{14}$$

with orthonormal discrete and continuum eigenfunctions satisfying the orthonormal relationships:

$$< \psi_k^n|\psi_l^n > = \delta_{kl},$$
$$< \psi_\sigma^n|\psi_\gamma^n > = \delta(\sigma - \gamma),$$
$$< \psi_k^n|\psi_\sigma^n > = 0.$$

3.2. The eigenvalue problem

In this subsection we tackle the eigenvalue problem

$$A[n]|\psi_\omega^n >= \omega^2|\psi_\omega^n >,$$

with boundary conditions

$$|\psi_\omega^n >_1 |_{x=0} = 0 = |\psi_\omega^n >_1 |_{x=1},$$

where $|\psi_\omega^n >_1$ is the first component of $|\psi_\omega^n >$. We have nondimensionalized lengths and speeds with respect to a and $v_A(0)$ respectively. To satisfy the boundary conditions, we expand $|\psi_\omega^n >_1$ (corresponding to ξ_x) as a Fourier sine series. The form of Eq. (12) then suggest that $|\psi_\omega^n >_2$ (corresponding to ξ_y) can be expanded in a cosine series:

$$|\psi_\omega^n >_1 (x) = \sum_{m=1}^{\infty}\alpha_m^n\sin(m\pi x),$$

$$|\psi_\omega^n >_2 (x) = \frac{1}{2}\beta_0^n + \sum_{m=1}^{\infty}\beta_m^n\cos(m\pi x).$$

Cally (1991) noted that for the density profile given by (1) the eigenvalue problem can be written as a single generalised matrix eigenvalue problem. We solve this eigenvalue problem by truncating the expansions to $m \leq N$: the $2N + 1$ eigenvalues and the coefficients α_m^n and β_m^n of the corresponding eigenvectors of the resulting *finite* matrix eigenvalue problem are easily found with the help of the NAGroutines F02FHF and F02SDF. With these eigenvalues and eigenvectors we can reconstitute the spectral representation (14). We refer to Appendix A of Mann, Wright & Cally (1995) for a description of the technical details for solving the eigenvalue problem.

This method has several advantages over more standard finite differencing schemes. Notably, by taking a sufficiently large number of Fourier modes, and following the propagation towards finer scales through resonant absorption and phase mixing, we can ensure that the structure of the waves is fully resolved at any time. In addition, we can compute the resolved

wave structures at any time by calculating the Fourier summation. This results in a considerable CPU-time saving in comparison with usual finite difference approaches, whereby the disturbance must be calculated at every previous timestep.

It has been checked that for the finite matrix eigenvalue problem the eigenfunctions remain orthogonal with respect to the scalar product (13). Hence as long as the finest scale in the x-direction of the MHD waves in the time evolution can be represented by $\sin(N\pi x)$ or $\cos(N\pi x)$, the spectral representation of $\hat{X}^{(n)}$ and $\hat{Y}^{(n)}$ can be adequately approximated by the sum over the discrete set of eigenfunctions of the finite generalised eigenvalue problem.

$$\hat{X}^{(n)}(x,\omega) = \sum_{m=1}^{N}\sum_{k=1}^{2N+1}\frac{\alpha^n_{mk}}{\omega_k^2-\omega^2} < \psi^n_k|B[n] > \sin(m\pi x), \tag{15}$$

$$\hat{Y}^{(n)}(x,\omega) = \frac{1}{2}\sum_{k=1}^{2N+1}\frac{\beta^n_{0k}}{\omega_k^2-\omega^2} < \psi^n_k|B[n] > + \sum_{m=1}^{N}\sum_{k=1}^{2N+1}\frac{\beta^n_{mk}}{\omega_k^2-\omega^2} < \psi^n_k|B[n] > \cos(m\pi x), \tag{16}$$

or in matrix notation

$$\begin{bmatrix}\hat{X}^{(n)}\\ \hat{Y}^{(n)}\end{bmatrix} = \sum_{k=1}^{2N+1}\frac{1}{\omega_k^2-\omega^2}|\psi^n_k >< \psi^n_k|B[n] > . \tag{17}$$

3.3. Inversion of transformations

We now want to invert the Laplace transform with respect to time and the sine transform with respect to z. For azimuthally polarised footpoint motions that can be described by a separable functions $R(x)T(t)$ the scalar product of the eigenfunctions and $B[n]$ reduces to

$$< \psi^n_k|B[n] >= \hat{T}(\omega)\{\frac{L}{n\pi}(\omega^2-\omega_k^2) < \psi^n_k|R(x) > + \frac{n\pi}{L}R^n_k\}, \tag{18}$$

where R^n_k is the scalar product without weightfunction of $R(x)$ and $|\psi^n_k >$

$$R^n_k = \int_0^1 R(x)|\psi^n_k(x) > dx.$$

Eq. (17) can then be written as

$$\begin{bmatrix}\hat{X}^{(n)}\\ \hat{Y}^{(n)}\end{bmatrix} = -\frac{L}{n\pi}R(x)\hat{T}(\omega) + \frac{n\pi}{L}\hat{T}(\omega)\sum_{k=1}^{2N+1}\frac{R^n_k}{\omega_k^2-\omega^2}|\psi^n_k > . \tag{19}$$

The Laplace-inversion of the first term of expression (19) is straightforward

$$-\frac{L}{n\pi}\hat{T}(\omega)R(x) \rightarrow -\frac{L}{n\pi}T(t)R(x)$$

To perform the Laplace inversion of the second term of expression (19) we first note that the complete ω-dependence is contained in the factor

$$\frac{\hat{T}(\omega)}{\omega_k^2-\omega^2}.$$

Secondly one should remember the well-known inversions

$$\frac{1}{\omega_k^2-\omega^2} \rightarrow \frac{\sin(\omega_k t)}{\omega_k},$$

$$\hat{f}_1(\omega)\hat{f}_2(\omega) \rightarrow \int_0^t f_1(t-\tau)f_2(\tau)d\tau.$$

Application of these two results enables us to invert

$$\frac{\hat{T}(\omega)}{\omega_k^2-\omega^2} \rightarrow \frac{1}{\omega_k}\int_0^t \sin(\omega_k(t-\tau))T(\tau)d\tau = T^n_k(t).$$

Plugging this time convolution into (18) we obtain

$$\begin{bmatrix}X^{(n)}\\ Y^{(n)}\end{bmatrix} = -\frac{L}{n\pi}R(x)T(t) + \frac{n\pi}{L}\sum_{k=1}^{2N+1}R^n_kT^n_k(t)|\psi^n_k > .$$

By recalling the definition of φ, the sine transformations and the half-range Fourier series for the eigenfunctions, we now can reconstruct the displacement components ξ_x and ξ_y as function of x, z and t

$$\xi_x(x,z,t) = \frac{2}{L}\sum_{n=1}^{\infty}\sum_{m=1}^{N}\{\frac{n\pi}{L}\sum_{k=1}^{2N+1}R^n_kT^n_k(t)\alpha^n_{mk}\}\sin(m\pi x)\sin(\frac{n\pi}{L}z) \tag{20}$$

$$i\xi_y(x,z,t) = \frac{2}{L}\sum_{n=1}^{\infty}\frac{n\pi}{L}\{\sum_{k=1}^{2N+1}R^n_kT^n_k(t)\frac{\beta^n_{0k}}{2} + \sum_{m=1}^{N}(\sum_{k=1}^{2N+1}R^n_kT^n_k(t)\beta^n_{mk})\cos(m\pi x)\}\sin(\frac{n\pi}{L}z), + R(x)T(t)\{1-\frac{z}{L}-\frac{2}{L}\sum_{n=1}^{\infty}\frac{L}{n\pi}\sin(\frac{n\pi}{L}z)\}, \tag{21}$$

where we omitted the trivial $e^{ik_y y}$ dependence. As a result of expression (9) the second term of (21) equals zero for all values of $z > 0$. However when $z = 0$ the second term equals $R(x)T(t)$ which is indeed the imposed azimuthally polarised footpoint motion.

Thus we have derived an analytical expression which describes the generation of linear MHD waves (coupled fast-Alfvén waves) by azimuthally polarised footpoint motions. The solution is written as a superposition of eigenmodes $|\psi^n_k >$ whose excitation is determined by the time dependence $T(t)$ of the footpoint motion through the convolution T^n_k and by the spatial dependence $R(x)$ of the footpoint motion through the scalar product R^n_k. This expression can be easily evaluated numerically at any time with the structure of the waves fully resolved

as long as a sufficiently large numbers of sines in both x and z directions are taken into account.

A combination of the expressions (20) and (21) with the results by Tirry, Berghmans & Goossens (1997) leads to in an analytical expression describing the generation of linear MHD waves by both radially polarised footpoint motion $R_x(x)T_x(t)$ and azimuthally polarised footpoint motions $R_y(x)T_y(t)$:

$$\begin{aligned}
&\xi_x(x,z,t) = \frac{2}{L}\sum_{n=1}^{\infty}\sum_{m=1}^{N} \qquad (22)\\
&\{\frac{n\pi}{L}\sum_{k=1}^{2N+1}(R^n_{xk}T^n_{xk}(t)+R^n_{yk}T^n_{yk}(t))\alpha^n_{mk}\}\\
&\times\sin(m\pi x)\sin(\frac{n\pi}{L}z)\\
&+R_x(x)T_x(t)\{1-\frac{z}{L}-\frac{2}{L}\sum_{n=1}^{\infty}\frac{L}{n\pi}\sin(\frac{n\pi}{L}z)\},\\
&i\xi_y(x,z,t) = \qquad (23)\\
&\frac{2}{L}\sum_{n=1}^{\infty}\frac{n\pi}{L}\{\sum_{k=1}^{2N+1}(R^n_{xk}T^n_{xk}(t)+R^n_{yk}T^n_{yk}(t))\frac{\beta^n_{0k}}{2}\\
&+\sum_{m=1}^{N}(\sum_{k=1}^{2N+1}(R^n_{xk}T^n_{xk}(t)+R^n_{yk}T^n_{yk}(t))\beta^n_{mk})\\
&\times\cos(m\pi x)\}\sin(\frac{n\pi}{L}z),\\
&+R_y(x)T_y(t)\{1-\frac{z}{L}-\frac{2}{L}\sum_{n=1}^{\infty}\frac{L}{n\pi}\sin(\frac{n\pi}{L}z)\},
\end{aligned}$$

where we again omitted the trivial $e^{ik_y y}$ dependence.

4. Temporal evolution of the resonance

In this section we use the solutions (20) and (21) to investigate how the coupling to the fast waves affects the temporal evolution of the resonant absorption and the associated phase-mixing. This will provide additional insight in the steady state results of Paper I. As in Paper I we consider the system described in Sect. 2 with $\rho_A = 0.6$, $\rho_B = 0.4$ and $L = 1$ corresponding to a range of Alfvén speeds of 1 (inside the loop) up to 2.24 (outside the loop) as an illuminating example (rather than a realistic model). In this paper we split up the constant profile of the footpoint driver used in Paper I into a footpoint driver which is localised around the resonant surface and the complementary driver. The localised footpoint driver will be referred to as the direct driver R_{dir} since it directly excites resonant Alfvén waves, while the complementary driver is referred to the indirect driver R_{ind} since Alfvén wave are resonantly excited through coupling with the fast waves:

$$R_{dir}(x) = \begin{cases} 0.01 & \text{for} \quad x_{res}-0.05 \le x \le x_{res}+0.05 \\ 0 & \text{elsewhere,} \end{cases}$$

$$R_{ind}(x) = \begin{cases} 0 & \text{for} \quad x_{res}-0.05 \le x \le x_{res}+0.05 \\ 0.01 & \text{elsewhere,} \end{cases}$$

$$T(t) = \begin{cases} \frac{1}{4}(\frac{t}{t_0})^2 e^{2-\frac{t}{t_0}} & \text{for} \quad t \le 2t_0 \\ \cos(\omega_d(t-2t_0)) & \text{for} \quad t > 2t_0, \end{cases}$$

where $t_0 = 0.2$ and x_{res} gives the location of the resonant surface. The t^2-dependence in the initial phase of $T(t)$ is included to guarantee that the initial conditions (6) are trivially fulfilled. In the first subsection the results for decoupled Alfvén waves ($k_y = 0$) are recapitulated. In the second subsection the influence of the coupling to the fast waves on the resonant Alfvén waves excited by azimuthally polarised footpoint motions is investigated.

4.1. Phase-mixing, resonances and beats

When $k_y = 0$ the Alfvén and fast waves are decoupled. Hence when the footpoint motions are purely azimuthal, only Alfvén waves are generated, propagating along the magnetic field lines with the local Alfvén speed. As the local Alfvén speed varies across the magnetic surfaces, the Alfvén waves on different surfaces become out of phase. This phase-mixing creates small length scales necessary for dissipation to become effective in the solar corona.

Due to the high conductivity and the relatively high mass density of the photosphere the Alfvén waves reflects back and forth along the length of the loop at the photospheric edges. When the driving frequency matches the local Alfvén eigenfrequency, a resonance is built up. In ideal MHD the amplitude at the resonant magnetic surface grows linearly in time. On the non-resonant surfaces beat phenomena are seen. The observed beat frequencies are in perfect agreement with the results mathematically found in analytical expressions e.g. by Berghmans & De Bruyne (1995).

It is obvious that the smaller the gradient across the magnetic surfaces in the Alfvén speed, the longer it takes for phase-mixing to generate the necessary small dissipative features. In the process of phase-mixing the typical length scale reduces proportional to the inverse of both time as the gradient in the Alfvén speed (see e.g. Mann, Wright & Cally, 1995)

$$L_{ph}(t) \sim \frac{1}{(\omega_A(x))'t} \qquad (24)$$

We first recover these results as a test but also as starting point for our investigation in the next subsection on how this physics is altered when the Alfvén waves are coupled to the fast waves (when $k_y \neq 0$).

Fig. 2 shows (a) the linear growth of the amplitude at the resonant surface $x = 0.671$ when the driving frequency $\omega_d = 5.0$, (b) the beat in the time evolution of the amplitude at the neighbouring surface $x = 0.6$, where the local Alfvén frequency $\omega_A(x = 0.6) = 4.55$. A constant profile $R(x)$ for the footpoint oscillation with $k_y = 0$ is used. The beat frequency $(\omega_d - \omega_A)/2$ shows up clearly. Fig. 3 shows the reduction in length scales due to the resonance and the phase mixing around the resonant position $x = 0.328$ for $\omega_d = 3.5$ with a small gradient in the Alfvén speed and at position $x = 0.671$ for $\omega_d = 5.0$ with a large gradient in the Alfvén speed.

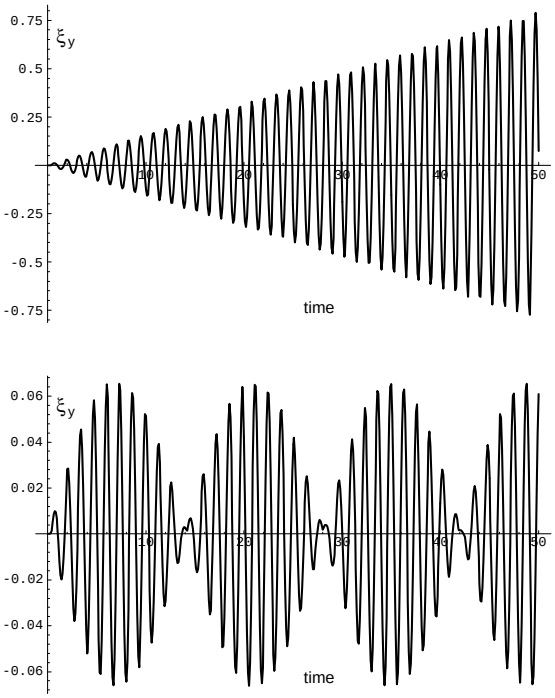

Fig. 2a and b. The amplitude of ξ_y (**a**) at the resonant surface as function of time, **b** at a neighbouring surface for $k_y = 0$ with the driving frequency $\omega_d = 5.0$.

Using a fit $\sim \frac{1}{t}$ we verified that the decrease in resonance length scale (defined as the full width at half of maximum height) is consistent with the expression (24) for the phase-mixing length scale.

The length of the loop has no influence on the rate of decrease in resonance length scale due to phase-mixing. It only affects the linear growth rate of the amplitude at the resonance position, and therefore the volumetric heating rate.

4.2. The influence of coupling to the fast waves

When $k_y \neq 0$, the Alfvén and fast waves do not exist any longer independently. The purely azimuthal footpoint motions now also generates indirectly a ξ_x component through coupling with the directly excited ξ_y component. When the frequency of the harmonic footpoint driver does not match an eigenfrequency of a discrete global mode (this means a driving frequency away from any quasi-mode frequency), one can expect that the coupling in case of the direct driver R_{dir} has a negative influence on the resonance growth at the magnetic surface where the driving frequency matches the local Alfvén frequency. Indeed, no global coherent wave motion can be built up due to destructive interference, which results in a smaller amplitude growth at the resonant surface for larger values of k_y. This can be seen in Fig. 4 where the driving frequency $\omega_d = 3.5$ and $k_y = 0, 1, 2, 4$. On the other hand the indirect driver R_{ind} now also excites resonant Alfvén waves through coupling with the ξ_x component. The phase difference between the contributions of the direct and indirect driver determines whether the coupling to the fast waves has a positive or negative influence on the resonance growth at the surface where the driving frequency matches the local Alfvén frequency.

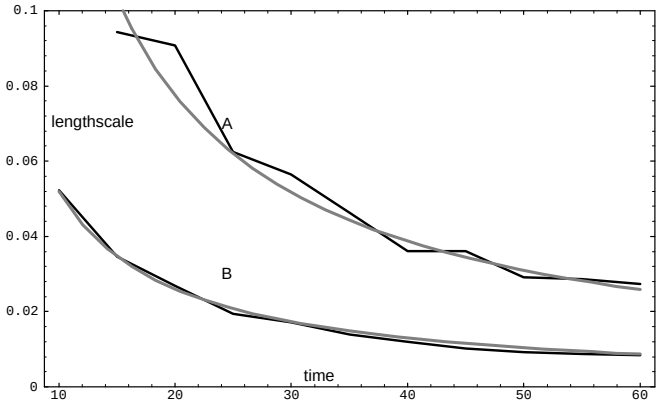

Fig. 3. The length scale of the resonance (defined as the full width at half of maximum height) as function of time. The length scale decreases proportional to the inverse of time as shown by the $1/t$ fits (dark gray lines). (A) corresponds to the resonance when $\omega_d = 3.5$, (B) to the resonance when $\omega_d = 5$.

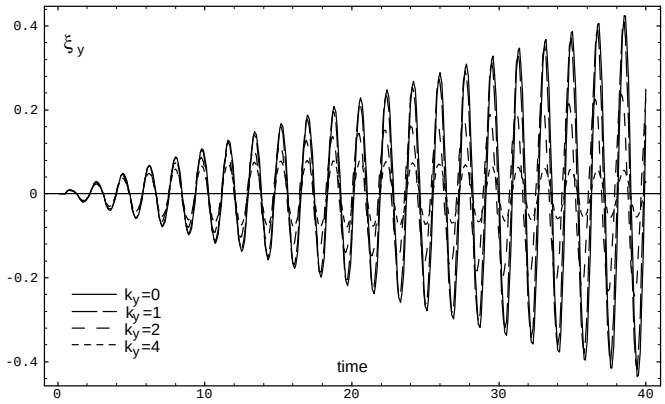

Fig. 4. The amplitude of ξ_y at the resonance as function of time for $k_y = 0, 1, 2, 4$ with the driving frequency $\omega_d = 3.5$.

The rate of decrease in resonance length scale is expected not to be influenced, since phase-mixing is the dominant process here. Fig. 5 shows the reduction in resonance length scale for $k_y = 0, 1, 2, 4$.

However when the driving frequency equals the oscillation frequency of a quasi-mode, a global wave motion is built up through coupling with the excited ξ_y wave component. The quasi-mode excites on its turn Alfvén waves on the resonant surface and hence looses its energy towards the resonance in correspondence with its damping rate. This means that the ξ_x component, which can be associated with the global behaviour in the quasi-mode, evolves to a stationary amplitude, as shown in Fig. 6 where $\omega_d = 5.471$ and $k_y = 2$. Fig. 7 shows the amplitude of ξ_y at the resonant surface. During an initial phase the global mode is built up towards his stationary state. Subsequently the

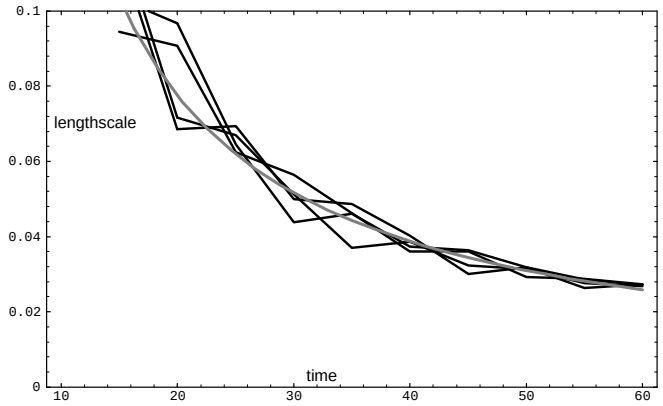

Fig. 5. The reduction of the length scale of the resonance in time with driving frequency $\omega_d = 3.5$ for $k_y = 0, 1, 2, 4$. The dark gray line corresponds to a $1/t$ fit.

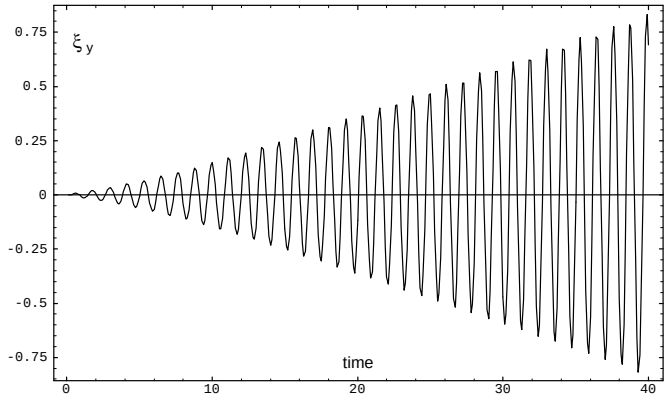

Fig. 7. The amplitude of ξ_y at the resonance as function of time for $k_y = 2$ with the driving frequency $\omega_d = 5.471$ the quasi-mode frequency.

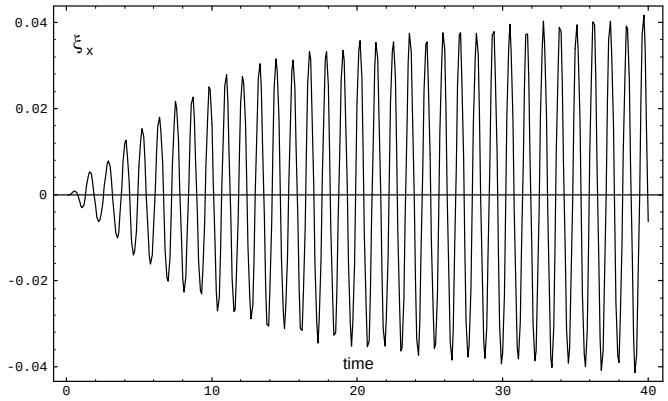

Fig. 6. The amplitude of ξ_x at the resonance as function of time for $k_y = 2$ with the driving frequency $\omega_d = 5.471$ the quasi-mode frequency.

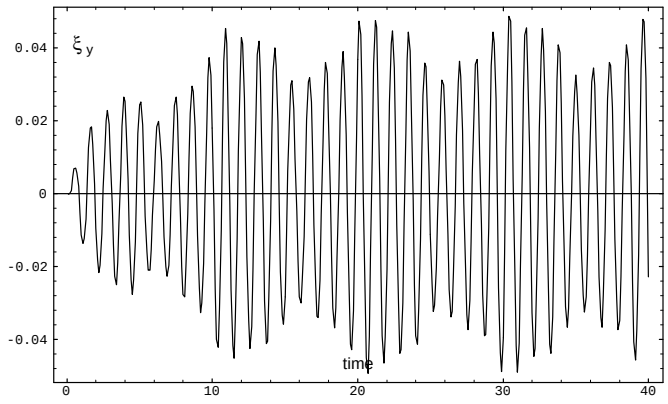

Fig. 8. The amplitude of ξ_y at a non resonant surface as function of time for $k_y = 2$ with the driving frequency $\omega_d = 5.471$ the quasi-mode frequency.

amplitude grows linearly in time according to two contributions: the direct excitation at the footpoints and the indirect excitation through coupling with the quasi-mode. On a non-resonant surface beating can be expected to, as in the case of pure Alfvén wave excitation ($k_y = 0$). The beating is modulated by the presence of the indirectly excited quasi-mode. Fig. 8 shows how the increase in the beats follows the increase of the amplitude of the quasi-mode in Fig. 5.

In the next three paragraphs we will consider different driving frequencies in the three different regions described in Paper I: $\omega_d = 5.72$ in region I, $\omega_d = 6.12$ in region II and $\omega_d = 5.84$ on the line that separates the two regions with $k_y = 2$.

$\omega_d = 6.12$. According to Paper I region I corresponds to combinations of frequencies and wave numbers with an energy inflow in the dissipative layer at the footpoints. Part of this energy is dissipated, the remaining part gets lost again through the photospheric edge outside the dissipative layer. Fig. 9 shows that a resonance is built up in both cases of direct and indirect driving. It is also clearly shown that the contributions are in opposite phase, but that the direct driving is dominant. Hence these results are consistent with the outcome of the steady state investigation in Paper I.

$\omega_d = 5.72$. According to Paper I region II corresponds to combinations of frequencies and wave numbers with an energy inflow from the photospheric edge ($z = 0$) outside the dissipative layer. Part of this energy is flowing out again through the photospheric edge at the dissipative layer. In Fig. 10 the time evolution of the amplitude of ξ_y at the resonance surface is plotted for the direct and indirect driver. In both cases a resonance growth is seen as expected. Comparing these time evolutions with the resulting Poynting fluxes in the steady state analysis in Paper I leads to the conclusion that the energy outflow from the dissipation layer at the photospheric part of the loop by the indirect excitation away from the resonant layer is not compensated by the inflow by excitation directly at the resonant surface.

$\omega_d = 5.84$. This frequency lies on the line that separates region I from region II, baptized as the 'anti-resonance line' in

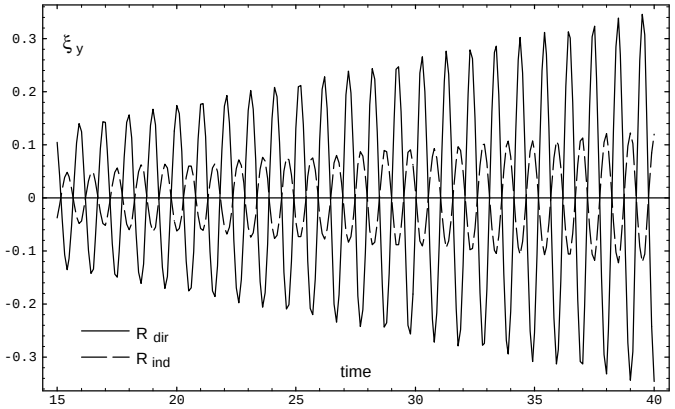

Fig. 9. The amplitude of ξ_y at the resonance as function of time for k_y = 2 with the driving frequency ω_d = 6.12 for the direct and indirect driver.

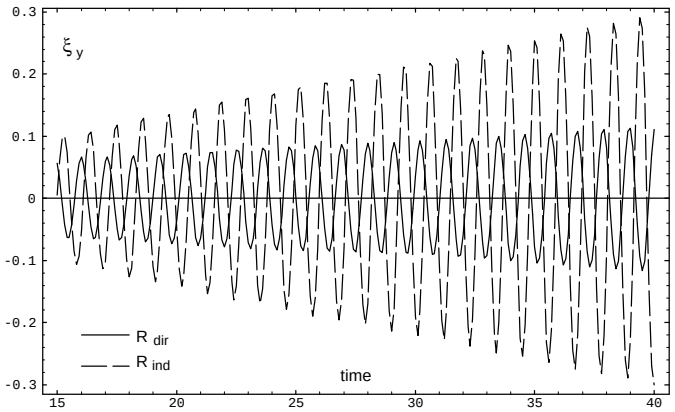

Fig. 10. The amplitude of ξ_y at the resonance as function of time for k_y = 2 with the driving frequency ω_d = 5.72 for the direct and indirect driver.

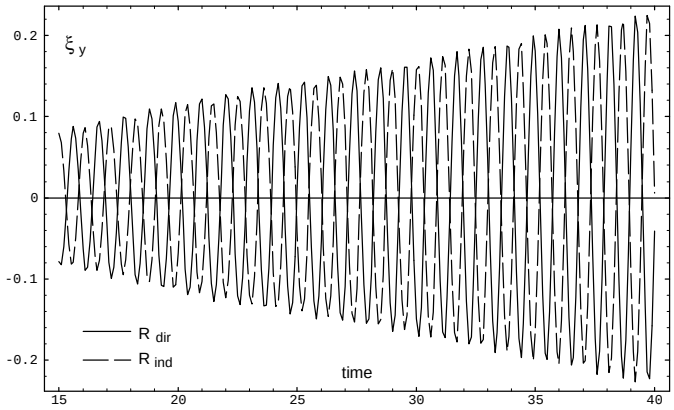

Fig. 11. The amplitude of ξ_y at the resonance as function of time for k_y = 2 with the driving frequency ω_d = 5.841 for the direct and indirect driver.

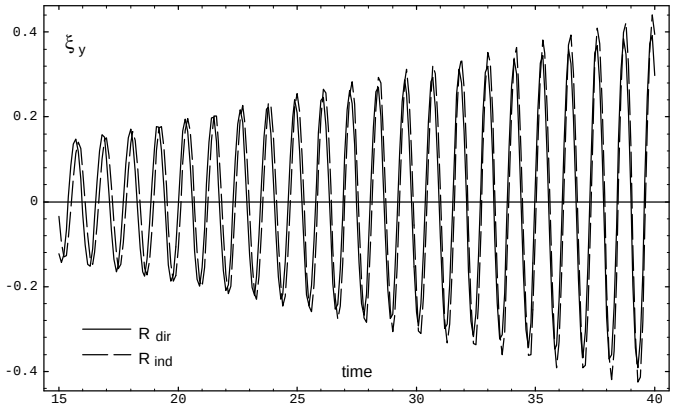

Fig. 12. The amplitude of ξ_y at the resonance as function of time for k_y = 2 with the quasi-mode frequency as the driving frequency ω_d = 6.12 for the direct and indirect driver.

Paper I. Hence there is no net inflow of energy in the loop. No resonance is built up at the surface where the local Alfvén frequency matches the driving frequency. The time evolution of the ξ_y component at the resonant surface is plotted in Fig. 11 for the indirect and the direct driving at the footpoints. Both contribute in the same amount to the resonance, but are in opposite phase. The only possibility in this case to dissipate energy is by creating small length scales by pure phase-mixing.

For completness we show in Fig. 12 the contributions of the direct and indirect driving in case of ω_d = 5.47 the quasi-mode frequency for k_y = 2. The contributions are of the same order and in phase as could be expected since the driving frequency matches an eigenfrequency of the system.

5. Diffusion time scales

For resonant absorption to be a viable heating mechanism for coronal loops the generation of small length scale should at least take place on time scales shorter than the lifetime of coronal loops. These time scales can be estimated from our ideal temporal simulations by expressing the dissipation time scale (function of the resonance length scale) as function of the physical time. Another requirement is that the resonant absorption of Alfvén waves provides the observed volumetric heating rates in coronal loops. The averaged observed energy fluxes are approximately $3 \times 10^2 W/m^2$ in the quiet corona up to $10^4 W/m^2$ in the active region loops (Hollweg 1990).

Imaging data from high resolution Normal-Incidence X-ray Telescope (NIXT) observations (Golub et al., 1990) reveal coronal loop dimensions in the ranges

$$2 \times 10^7 \mathrm{m} \leq\ L\ \leq 2 \times 10^8 \mathrm{m}$$
$$4 \times 10^5 \mathrm{m} \leq\ a\ \leq 4 \times 10^6 \mathrm{m}$$

A typical Alfvén speed in the solar corona is of the order of 10^6m/s so that the Alfvén transit time along the loop varies, let say, from 5 to 100 seconds. For larger Alfvén transit times it takes longer for the resonantly excited Alfvén waves to interfere constructively. The amplitude at the resonance scales proportional to the inverse of the loop length. From the paper by

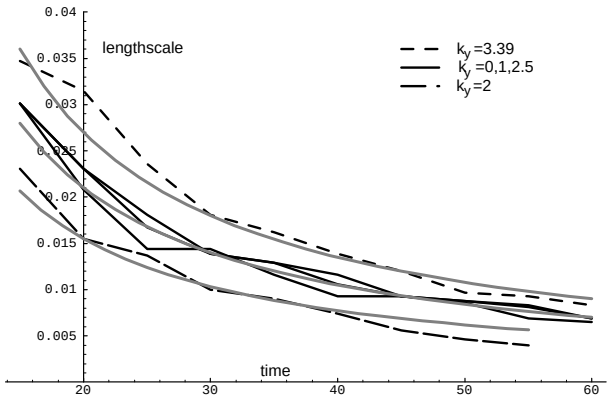

Fig. 13. The reduction of the length scale of the resonance in time with driving frequency $\omega_d = 5.841$ for different values of $k_y = 0, 1, 2, 2.5, 3.39$ corresponding with the different regions discussed in Paper I. The dark gray lines correspond to $1/t$ fits.

Tirry, Berghmans & Goossens (1997) where the excitation with radially polarised footpoint motions is considered, we know that once the global mode is excited, the length of the loop is not involved in the generation of small length scales in the radial direction by the resonant absorption of Alfvén waves, but of course it is important for the volumetric heating rate. The phase-mixing process is also not influenced by the length of the loop. Hence we can assume that in case of excitation with azimuthally polarised footpoint motions the length of the loop has also no influence on the decrease in resonance length scale. This result allows us to investigate the reduction of the length scale corresponding to the resonance with small values of L which saves a lot of CPU time.

In plasmas, the diffusion time scales depend on the typical length scale. We will use the resistive diffusion time scale τ_{dif} to estimate the time when dissipation becomes important and thus our ideal MHD simulations stop to be valid. The resistive diffusion time scale is estimated as l^2/η, where l denotes a typical length scale and η denotes the magnetic diffusivity. For the solar coronal conditions, the magnetic diffusivity η is of the order of 1 m^2/s (Priest, 1987) so that $\tau_{dif} \sim l^2$. Typical life times of coronal loops vary from 6 to 24 hours. For dissipation to become important the dissipation time scale should be reduced less than the half of the life time of the coronal loop. This means that length scales about 100 meter should be generated within half of the life time of the coronal loop. Fig. 13 shows the reduction in resonance length scale for $\omega_d = 5.84$ for different values of $k_y = 0, 1, 2, 2.5, 3.39$ corresponding to the different regions discussed in Paper I. For $k_y = 2$ (on the line between region I and region II the decrease of the phase-mixing length scale goes faster than the inverse of time, while for the other values of k_y the reduction in resonance length scale goes approximately proportional to the inverse of time. In the case of driving with the quasi-mode frequency the decrease is the slowest. But even in this case the time needed to generate a length scale about 100 meter lies between 2 and 3 hours, estimated using the fit $l = 0.6 \times 10^6/t$. So dissipation seems to become important in a time of the order of the life time of the loop. This is a rather rough estimation, but certainly not an overestimation in linear theory. Hence at first sight it looks as if the necessary dissipative small length scales are created sufficiently fast, resulting in a substantial heating of the coronal loop. Numerical nonlinear simulations by Ofman & Davila (1995) show that the highly sheared velocities at the narrow resonance layer are subject to a Kelvin-Helmholtz like instability. They also found that the resonant absorption heating layers are not destroyed by the Kelvin-Helmholtz instability. This instability may lead to turbulent enhancement of the dissipation parameters and acceleration to smaller length scales (Hollweg & Yang 1988) and account for the observed turbulent velocities inferred from the onthermal broadening of X-ray and EUV emission lines.

It is important to note that the steady state solutions with relatively high dissipation rates corresponding to locations of small gradient in Alfvén speed (see Paper I: $|\Delta| \ll 1$) never will be attained since the phase mixing length scale decrease inverse proportional to ω_A'. Hence it seems fair to conclude that the resonant absorption of Alfvén waves directly excited by azimuthally polarised footpoint motions at resonant places of relatively high gradient in Alfvén speed with or without coupling to the quasi-mode generates the small length scales necessary for coronal heating in time.

6. Summary and discussion

By considering an instructive example (rather than a realistic model for a coronal loop) the influence of the coupling to the fast waves on the resonant Alfvén waves excited by azimuthally polarised footpoint motion is investigated. We modelled a coronal loop as a straight, static plasma slab, obeying the set of ideal MHD equations in the zero-β-approximation. In this approximation we were able to write the general solution for the temporal evolution of the excited linear MHD waves as a superposition of eigenmodes (representing coupled Alfvén-fast waves) where the time dependence of the footpoint motion enters in the expressions through convolutions and the radial dependence of the footpoint motion through scalar products. The analytical solution can be easily evaluated numerically at any time with the structure of the waves being resolved as long as a sufficient number of sines in both the x and z direction are taken into account.

We have split up the driver used in the dissipative steady state investigation (Paper I) into a direct driver, which drives directly Alfvén waves at the footpoint of the resonant surface, and an indirect driver, which excites Alfvén waves through coupling with the fast waves. When $k_y \neq 0$ both drivers excite a resonance at the surface where the driving frequency matches the local Alfvén frequency. The phase difference between and the efficiency of these two ways of driving resonant Alfvén waves determine whether the coupling to the fast waves has a positive or negative influence on the resonance depending on the combination of the values of the wave number k_y and the driving frequency. We have seen that it is possible that both contribute in the same amount to the resonance, but are in opposite phase,

so that there is actually no resulting resonance. On the other hand, at a quasi-mode frequency, both contributions are of the same order and in phase, as might expected for driving with an eigenfrequency. This way of looking at the ratio of and the phase difference between the direct and indirect contribution helped to understand the figures of average energy flow of Paper I.

It is shown that the length scales of the resonance are reduced proportional to the inverse of time as in the case of sideways excitation and excitation by radially polarised footpoint motions. However for the combination of frequency and wave number where the resonances of the direct and indirect driving cancel each other, the phase-mixing length scale decreases faster than the inverse of time as in the case of pure Alfvén wave excitation ($k_y = 0$).

The simulations are carried out in ideal MHD. Nonetheless, we can estimate by following the dissipation time scale (corresponding to the resonance length scale) as function of the physical time, a time when dissipation would start to become important. This rather rough estimation (but certainly not an overestimation) leads us to conclude that in linear MHD dissipation becomes important in a time scale comparable to the life time of the coronal loops.

The Kelvin-Helmholtz instability due to the highly sheared velocities at the narrow resonance layer may lead to turbulent enhancement of the dissipation parameters and an acceleration to smaller length scales (Hollweg & Yang 1988; Ofman & Davila 1995). Under this assumption we can state that direct excitation of Alfvén waves at surfaces of relatively large gradient of Alfvén speed,with or without a global mode, by azimuthally polarised footpoint motions develops small enough dissipative features in acceptable time scales.

In the analysis towards the general solution for the temporal evolution of the excited linear MHD waves as a superposition of eigenmodes the spatial variation $R(x)$ and the time dependence $T(t)$ of the footpoint motion can be chosen arbitrarily. This allows us to extend the study towards driving with pulses, wavepackets, wave trains of pulses, randomly as more realistic models for the photospheric turbulent motion and for wave generation by microflaring. This will be done in a future study.

Acknowledgements. The authors are grateful to M. Goossens for his suggestion to undertake this work. We also gratefully acknowledge the valuable discussions with S. Poedts and M.S. Ruderman.

References

Berghmans, D., & De Bruyne, P. 1995, ApJ, 453, 495
Berghmans, D., De Bruyne, P., & Goossens, M. 1996, ApJ, 472, to appear
Berghmans, D., & Tirry, W.J. 1996, A&A, accepted
Cally, P.S. 1991, J. Plasma Phys., 45, 453
Cheng, C.C., Doschek, G.A., & Feldman, U. 1979, ApJ, 227, 1037
Falconer, D.A., Moore, R.L., Porter, J.G., Gary, G.A., & Shimizu, T. 1996, ApJ, in press
Goedbloed, J.P. 1994, International Conference on Plasma Physics, in press
Golub, L., Herant, M., Kalata, K., Louas, I., Nystrom, G., Pardo, F., Spiller, E., & Wilczynski, J. 1990, Nat, 344, 842
Goossens, M., Ruderman, M.S., & Hollweg, J.V. 1995, SPh, 157, 75
Goossens, M., & Ruderman, M.S., 1995, Physica Scripta, Vol T60, 171
Halberstadt, G., & Goedbloed, J.P. 1995a, A&A, 301, 559
Halberstadt, G., & Goedbloed, J.P. 1995b, A&A, 301, 577
Hollweg, J.V. 1984, ApJ, 277, 392
Hollweg, J.V., & Yang, G. 1988, J. Geophys. Res., 93, 5423
Hollweg, J.V. 1990, Comp. Phys. Rep., 12, 205
Mann, I.R., Wright, A.N., & Cally, P.S. 1995, J. Geophys. Res., 100, 19441
Ofman, L., & Davila, J.M. 1995, J. Geophys. Res., 100, 23427
Ofman, L., & Davila, J.M. 1996, Astrophys. Lett., 456, L123
Parker, E.N. 1972, ApJ, 174, 499
Parker, E.N. 1992, J. Geophys. Res., 97, 4311
Poedts, S., Goossens, M., & Kerner, W. 1989, Solar Phys., 123, 83
Poedts, S., & Kerner, W. 1991, Phys. Rev. Lett., 66, 22
Poedts, S., & Kerner, W. 1992, J. Plasma Phys., 47(1), 139
Poedts, S., Beliën, A.J.C., & Goedbloed, J.P. 1994, Solar Phys., 151, 271
Poedts, S., & Boynton, G.C. 1996, A&A, 306, 610
Priest, E.R. 1987, Solar Magnetohydrodynamics, D. Reidel Publishing
Ruderman, M.S., Berghmans, D., Goossens, M., & Poedts, S. 1996, A&A, accepted
Saba, J.L.R., & Strong, K.T. 1991, ApJ, 375, 789
Steinolfson, R.S., & Davila, J.M. 1993, ApJ, 415, 354
Tirry, W.J., & Goossens, M. 1996, ApJ, 471, 501
Tirry, W.J., Berghmans, D., & Goossens, M. 1997, A&A, accepted
Ulrich, R.K. 1996, ApJ, accepted
Van Ballegooijen, A.A. 1985, ApJ, 298, 421
Wright, A.N., & Rickard, G.J. 1995, ApJ, 444, 458
Zirker, J.B. 1993, Solar Phys., 148, 43

This article was processed by the author using Springer-Verlag LaTeX A&A style file *L-AA* version 3.